Chapter 2
Time-Varying Inverse Square Root

Abstract In this chapter, we propose, generalize, develop, and investigate different ZD models based on different ZFs for solving the time-varying inverse square root problem. In addition, this chapter shows modeling of the proposed ZD models using MATLAB Simulink techniques. The modeling results with different illustrative examples further substantiate the efficacy of such proposed ZD models for time-varying inverse square root finding.

2.1 Introduction

Inverse square root computation is an important numerical operation in many application areas such as digital signal processing, scientific computing, and computer graphics [1]. Specifically, inverse square root computation of a floating point scalar is exploited to compute a normalized vector [2], which can be used to determine lighting and reflection in a 3D graphics program [3]. The static inverse square root problem is generally formulated as $f(x) = ax^2 - 1$. Numerous numerical algorithms are investigated for solving such a problem [4–8]. Note that many potential computational algorithms are designed intrinsically for static (or to say, time-invariant, constant) problems solving [4] and associated with gradient methods [9]. As a result, almost all the previous algorithms are just effective for static inverse square root computation [10], and may not be accurate enough to solve the time-varying inverse square root problem [11–13].

In this chapter, focusing on time-varying inverse square root finding, we propose, generalize, develop, and investigate different ZD models by defining different ZFs as the error-monitoring functions. In addition, theoretical results are presented to show the convergence performance of such different ZD models. Moreover, MATLAB Simulink modeling [14–16] is shown for possible hardware realization of the proposed ZD models. Illustrative examples and modeling results further substantiate the efficacy of such proposed ZD models for time-varying inverse square root finding.

Y. Zhang and D. Guo, *Zhang Functions and Various Models*,
DOI 10.1007/978-3-662-47334-4_2

2.2 ZFs and ZD Models

In this section, different ZFs are introduced to construct different ZD models for time-varying inverse square root finding.

Let us consider the time-varying inverse square root problem, which is written in the form [11–13]

$$f(x(t), t) = a(t)x^2(t) - 1 = 0 \in \mathbb{R}, \ t \in [0, +\infty), \tag{2.1}$$

where $a(t) > 0 \in \mathbb{R}$ denotes a smoothly time-varying scalar with $\dot{a}(t) \in \mathbb{R}$ denoting the time derivative of $a(t)$, both of which are assumed to be known numerically or could be measured accurately. In this chapter, we aim at finding the $x(t) \in \mathbb{R}$ at time instant $t \in [0, +\infty)$ to make (2.1) hold true. Furthermore, $x^*(t)$ is used to denote the theoretical time-varying inverse square root of $a(t)$ [i.e., mathematically, $x^*(t) = \pm 1/\sqrt{a(t)}$] in this chapter.

For solving the time-varying inverse square root problem (2.1), different ZD models based on different ZFs are thus developed and investigated, with the corresponding design procedures detailed as follows.

2.2.1 The First ZF and ZD Model

Following Zhang et al.'s design method [11–15, 17] (see also Sect. 1.2), we define the following indefinite ZF (i.e., the first ZF) as the error-monitoring function for time-varying inverse square root finding:

$$e(t) = x^2(t) - \frac{1}{a(t)}. \tag{2.2}$$

With ZF (2.2), by expanding the ZD design formula (1.2), we obtain

$$2x(t)\dot{x}(t) + \frac{1}{a^2(t)}\dot{a}(t) = -\gamma\left(x^2(t) - \frac{1}{a(t)}\right).$$

Hence, the ZD model based on ZF (2.2) for time-varying inverse square root finding is derived as follows:

$$\dot{x}(t) = -\frac{\dot{a}(t)}{2a^2(t)x(t)} - \frac{1}{2}\gamma\left(x(t) - \frac{1}{a(t)x(t)}\right). \tag{2.3}$$

Correspondingly, the block diagram of ZD model (2.3) is shown in the upper graph of Fig. 2.1.

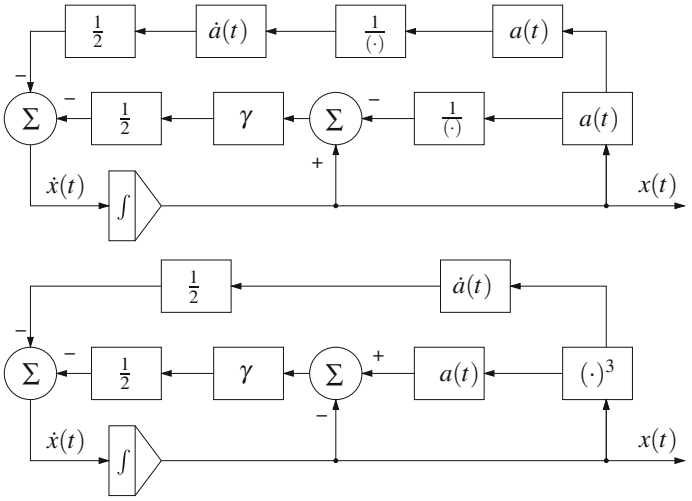

Fig. 2.1 Block diagrams of ZD (2.3) and (2.5) for time-varying inverse square root finding

2.2.2 The Second ZF and ZD Model

To introduce and show different ZD models based on different ZFs for solving the time-varying inverse square root problem (2.1), the second ZF is defined as

$$e(t) = a(t) - \frac{1}{x^2(t)}. \tag{2.4}$$

In view of ZF (2.4) and the ZD design formula (1.2), we obtain

$$\dot{a}(t) + \frac{2}{x^3(t)}\dot{x}(t) = -\gamma\left(a(t) - \frac{1}{x^2(t)}\right).$$

That is,

$$\dot{x}(t) = -\frac{1}{2}\dot{a}(t)x^3(t) - \frac{1}{2}\gamma\left(a(t)x^3(t) - x(t)\right), \tag{2.5}$$

which is the ZD model based on ZF (2.4) for time-varying inverse square root finding. Correspondingly, the block diagram of ZD model (2.5) is depicted in the lower graph of Fig. 2.1.

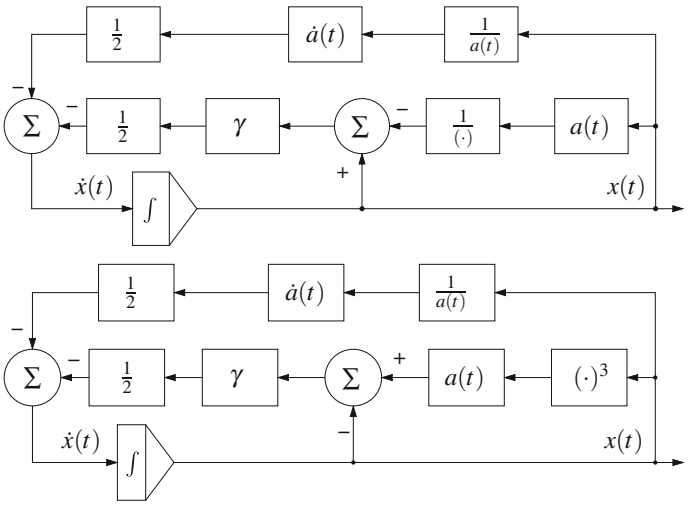

Fig. 2.2 Block diagrams of ZD (2.7) and (2.9) for time-varying inverse square root finding

2.2.3 The Third ZF and ZD Model

The first ZF (2.2) and the second ZF (2.4), which lead to ZD models (2.3) and (2.5), respectively, are defined above. Now, alternatively, we define the third ZF as

$$e(t) = a(t)x^2(t) - 1. \tag{2.6}$$

In view of the ZD design formula (1.2) and ZF (2.6), we have

$$\dot{a}(t)x^2(t) + 2a(t)x(t)\dot{x}(t) = -\gamma\left(a(t)x^2(t) - 1\right),$$

which is further written as

$$\dot{x}(t) = -\frac{\dot{a}(t)x(t)}{2a(t)} - \frac{\gamma}{2}\left(x(t) - \frac{1}{a(t)x(t)}\right). \tag{2.7}$$

Correspondingly, the block diagram of ZD model (2.7) for time-varying inverse square root finding is depicted in the upper graph of Fig. 2.2.

2.2.4 The Fourth ZF and ZD Model

For monitoring and controlling the process of the time-varying inverse square root problem (2.1) solving, another ZF (i.e., the fourth ZF) is defined in the following form:

$$e(t) = \frac{1}{a(t)x^2(t)} - 1. \tag{2.8}$$

With the ZD design formula (1.2) and ZF (2.8) considered, we have

$$-\frac{\dot{a}(t)x(t) + 2a(t)\dot{x}(t)}{a^2(t)x^3(t)} = -\gamma\left(\frac{1}{a(t)x^2(t)} - 1\right),$$

which yields the following differential equation of ZD:

$$\dot{x}(t) = -\frac{\dot{a}(t)x(t)}{2a(t)} - \frac{\gamma}{2}\left(a(t)x^3(t) - x(t)\right). \tag{2.9}$$

Correspondingly, the block diagram of ZD model (2.9) is shown in the lower graph of Fig. 2.2.

2.2.5 The Fifth ZF and ZD Model

Let us consider the following error-monitoring function (i.e., the fifth ZF):

$$e(t) = x(t) - \frac{1}{a(t)x(t)}. \tag{2.10}$$

As another form of ZF for time-varying inverse square root finding, ZF (2.10) leads to a different ZD model. Specifically, expanding the ZD design formula (1.2) with the aid of ZF (2.10), we obtain

$$\dot{x}(t) + \frac{\dot{a}(t)x(t) + a(t)\dot{x}(t)}{a^2(t)x^2(t)} = -\gamma\left(x(t) - \frac{1}{a(t)x(t)}\right),$$

which yields the following differential equation of ZD:

$$\dot{x}(t) = -\frac{\dot{a}(t)x(t)}{a^2(t)x^2(t) + a(t)} - \gamma\frac{a(t)x^3(t) - x(t)}{a(t)x^2(t) + 1}. \tag{2.11}$$

2.2.6 The Sixth ZF and ZD Model

The sixth and also the last ZF is given finally as

$$e(t) = a(t)x(t) - \frac{1}{x(t)}. \tag{2.12}$$

Table 2.1 Different ZFs resulting in different ZD models for finding time-varying inverse square root

ZF	ZD model
(2.2)	$\dot{x}(t) = -\frac{\dot{a}(t)}{2a^2(t)x(t)} - \frac{1}{2}\gamma\left(x(t) - \frac{1}{a(t)x(t)}\right)$
(2.4)	$\dot{x}(t) = -\frac{1}{2}\dot{a}(t)x^3(t) - \frac{1}{2}\gamma\left(a(t)x^3(t) - x(t)\right)$
(2.6)	$\dot{x}(t) = -\frac{\dot{a}(t)x(t)}{2a(t)} - \frac{1}{2}\gamma\left(x(t) - \frac{1}{a(t)x(t)}\right)$
(2.8)	$\dot{x}(t) = -\frac{\dot{a}(t)x(t)}{2a(t)} - \frac{1}{2}\gamma\left(a(t)x^3(t) - x(t)\right)$
(2.10)	$\dot{x}(t) = -\frac{\dot{a}(t)x(t)}{a^2(t)x^2(t)+a(t)} - \gamma\frac{a(t)x^3(t)-x(t)}{a(t)x^2(t)+1}$
(2.12)	$\dot{x}(t) = -\frac{\dot{a}(t)x^3(t)}{a(t)x^2(t)+1} - \gamma\frac{a(t)x^3(t)-x(t)}{a(t)x^2(t)+1}$

Substituting ZF (2.12) into the ZD design formula (1.2), we have

$$\dot{a}(t)x(t) + a(t)\dot{x}(t) + \frac{\dot{x}(t)}{x^2(t)} = -\gamma\left(a(t)x(t) - \frac{1}{x(t)}\right),$$

which yields the following differential equation of ZD:

$$\dot{x}(t) = -\frac{\dot{a}(t)x^3(t)}{a(t)x^2(t)+1} - \gamma\frac{a(t)x^3(t)-x(t)}{a(t)x^2(t)+1}. \tag{2.13}$$

Due to similarity to the block diagrams of the previous ZD models, the block diagrams of ZD models (2.11) and (2.13) are omitted.

In summary, we have obtained six different ZD models [i.e., (2.3), (2.5), (2.7), (2.9), (2.11) and (2.13)] for solving the time-varying inverse square root problem (2.1). Such six ZD models are derived from six different ZFs (2.2), (2.4), (2.6), (2.8), (2.10) and (2.12), respectively. For comparison purposes and reading convenience, the proposed different ZD models based on different ZFs are listed in Table 2.1.

2.3 Theoretical Results and Analyses

In this section, theoretical results and analyses are presented, which show the convergence properties of the proposed ZD models (2.3), (2.5), (2.7), (2.9), (2.11) and (2.13) for finding time-varying inverse square root.

Proposition 2.1 *Consider a smoothly time-varying positive scalar* $a(t) > 0 \in \mathbb{R}$ *involved in (2.1). Starting from any initial state* $x(0) \neq 0 \in \mathbb{R}$*, we have*

- *if $x(0) > 0$, the neural state $x(t) \in \mathbb{R}$ of ZD model (2.3) based on ZF (2.2) converges to the positive theoretical time-varying inverse square root of $a(t)$, with ZF (2.2) exponentially converging to zero; and,*
- *if $x(0) < 0$, the neural state $x(t) \in \mathbb{R}$ of ZD model (2.3) based on ZF (2.2) converges to the negative theoretical time-varying inverse square root of $a(t)$, with ZF (2.2) exponentially converging to zero.*

Proof We use the well-known Lyapunov theory to prove the convergence performance of ZD model (2.3).

Let us first define the following Lyapunov function candidate, which is clearly nonnegative:

$$V(x(t), t) = \frac{1}{2}\left(x^2(t) - \frac{1}{a(t)}\right)^2 \geqslant 0,$$

where $V(x(t), t) = 0$ only if $x(t) = x^*(t) = \pm 1/\sqrt{a(t)}$ and $V(x(t), t) > 0$ if $x(t) \neq x^*(t) = \pm 1/\sqrt{a(t)}$. In addition, if $e(t) = x^2(t) - 1/a(t)$ tends to infinity [correspondingly $|x(t) - x^*(t)| \to \infty$], we have $V(x(t), t) \to \infty$ as well.

Then, along the state trajectory of ZD model (2.3), we derive the time derivative of $V(x(t), t)$ as

$$\begin{aligned}\dot{V}(x(t), t) = \frac{\mathrm{d}V(x(t), t)}{\mathrm{d}t} &= \left(x^2(t) - \frac{1}{a(t)}\right)\left(2x(t)\dot{x}(t) + \frac{1}{a^2(t)}\dot{a}(t)\right) \\ &= -\gamma\left(x^2(t) - \frac{1}{a(t)}\right)^2 = -2\gamma V(x(t), t) \leqslant 0,\end{aligned}$$

which guarantees the final negative-definiteness of $\dot{V}(x(t), t)$.

Thus, in accordance with the Lyapunov theory, $x(t)$ converges to $x^*(t)$. In addition, as seen from the dynamic equation of ZD model (2.3), zero cannot be a divisor, i.e., state $x(t) \neq 0$. In view of the solution continuity of ZD model (2.3), we obtain the following results. If initial state $x(0) > 0$, the neural state $x(t) \in \mathbb{R}$ of ZD model (2.3) converges to the positive theoretical time-varying inverse square root of $a(t)$, i.e., $x(t) \to x^*(t) = 1/\sqrt{a(t)}$. Otherwise [i.e., if initial state $x(0) < 0$], the neural state $x(t) \in \mathbb{R}$ of ZD model (2.3) converges to the negative theoretical time-varying inverse square root of $a(t)$, i.e., $x(t) \to x^*(t) = -1/\sqrt{a(t)}$.

Furthermore, from $\dot{V}(x(t), t) = -2\gamma V(x(t), t)$, we have

$$V(x(t), t) = V(x(0), 0)\exp(-2\gamma t).$$

That is,

$$\frac{1}{2}\left(x^2(t) - \frac{1}{a(t)}\right)^2 = \frac{1}{2}\left(x^2(0) - \frac{1}{a(0)}\right)^2 \exp(-2\gamma t).$$

Thus, we have

$$\left|x^2(t) - \frac{1}{a(t)}\right| = \left|x^2(0) - \frac{1}{a(0)}\right| \exp(-\gamma t).$$

By setting $\alpha = |x^2(0) - 1/a(0)|$, the above equation becomes

$$\left|x^2(t) - \frac{1}{a(t)}\right| = \alpha \exp(-\gamma t),$$

which indicates that $x^2(t)$ exponentially converges to $1/a(t)$, i.e., ZF (2.2) exponentially converges to zero. Therefore, the proof is complete. □

As for the other five ZD models, we also have the corresponding convergence results. Concerning the convergence performance of the proposed ZD models based on six different ZFs, the following unified proposition is presented, with the related proof being generalized from the proof of Proposition 2.1 and being left to interested readers to complete as a topic of exercise.

Proposition 2.2 *Consider a smoothly time-varying positive scalar $a(t) > 0 \in \mathbb{R}$ involved in (2.1). Starting from any initial state $x(0) \neq 0 \in \mathbb{R}$,*

- *if $x(0) > 0$, the neural states $x(t) \in \mathbb{R}^+$ of ZD models listed in Table 2.1 converge to the positive theoretical time-varying inverse square root of $a(t)$, with ZFs listed in Table 2.1 exponentially converging to zero, respectively; and,*
- *if $x(0) < 0$, the neural states $x(t) \in \mathbb{R}^-$ of ZD models listed in Table 2.1 converge to the negative theoretical time-varying inverse square root of $a(t)$, with ZFs listed in Table 2.1 exponentially converging to zero, respectively.*

2.4 Simulink Modeling

In this section, the MATLAB Simulink modeling of the proposed ZD models [i.e., (2.3), (2.5), (2.7), (2.9), (2.11) and (2.13)] is investigated and presented. The overall Simulink models of such proposed ZD models for time-varying inverse square root finding are shown in Figs. 2.3 and 2.4.

Some important parameters and options related to the Simulink models which we establish in Figs. 2.3 and 2.4, etc., are specified as follows.

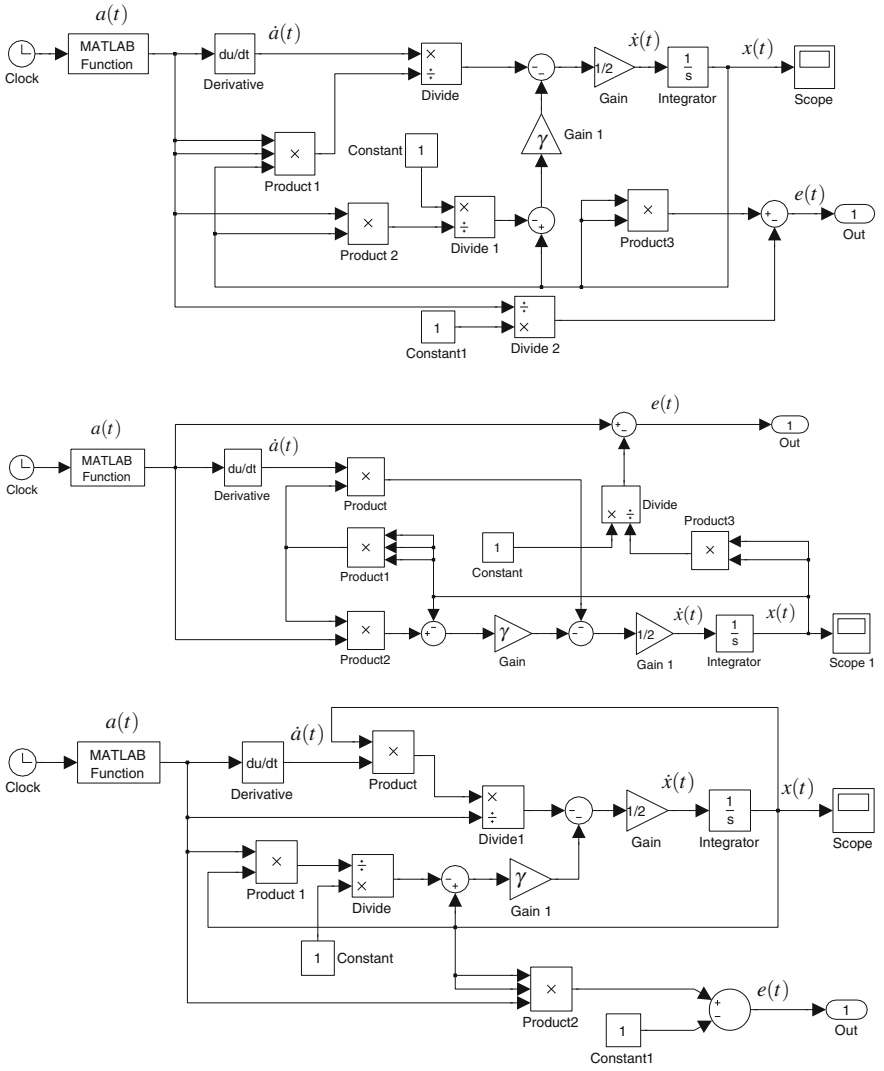

Fig. 2.3 Modeling of ZD (2.3), (2.5) and (2.7) for finding time-varying inverse square root

- $a(t)$ is generated by employing the "MATLAB Function" block with the "Clock" block as its input.
- Open the "Configuration Parameters" dialog box and set the options "Solver" to be "ode15s", "Max step size" to be "0.1", and "Min step size" to be "auto". In addition, by default, the option "Relative tolerance" is set as "1e-5" (i.e., 10^{-5}), and "Absolute tolerance" is "auto".

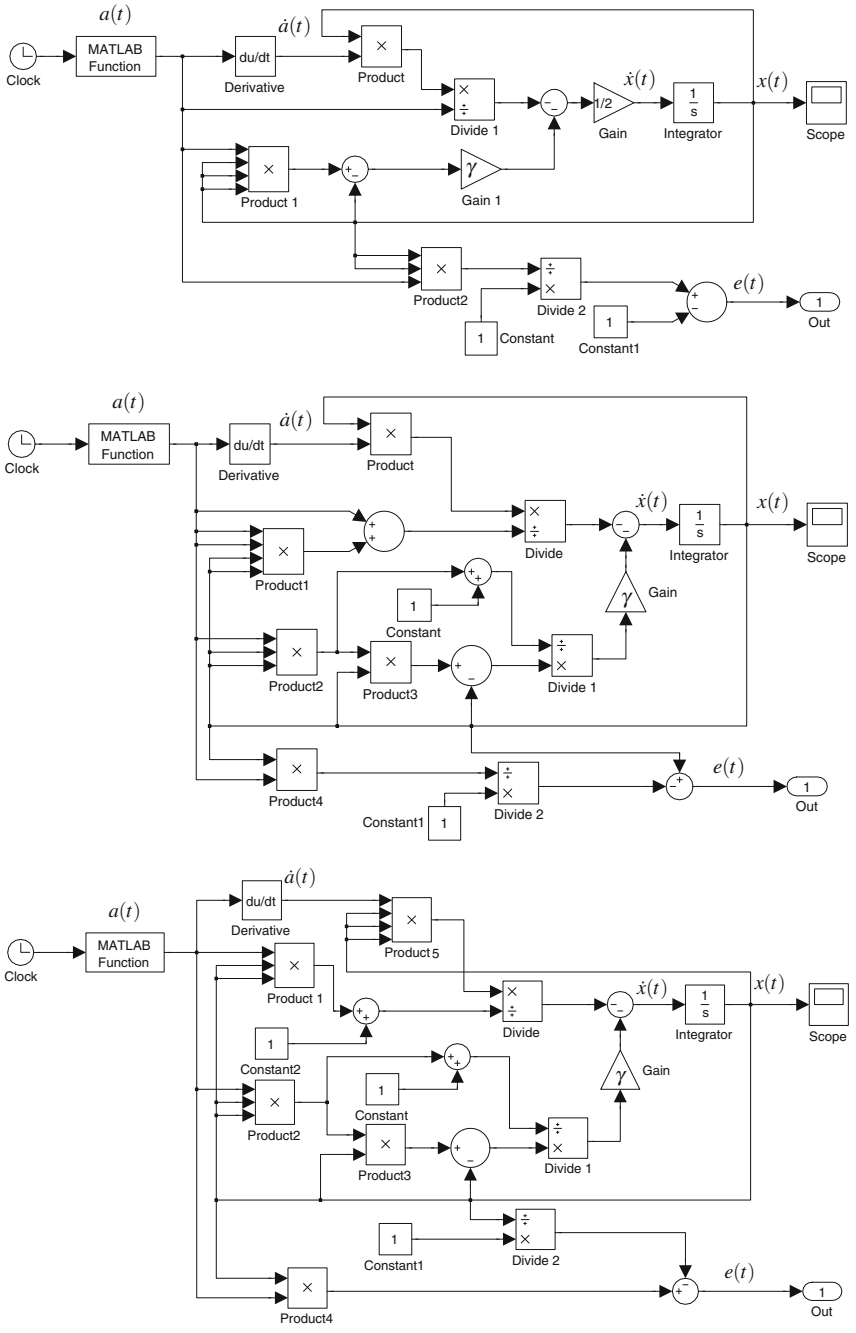

Fig. 2.4 Modeling of ZD (2.9), (2.11) and (2.13) for time-varying inverse square root finding

2.5 Illustrative Examples

In this section, based on the MATLAB Simulink modeling techniques, we substantiate the convergence performance of the proposed ZD models through two examples.

Example 2.1 Let us consider the time-varying inverse square root problem (2.1) with $a(t) = 8\cos(\sin(5t)) + 3\sin(2t) + 1$; i.e.,

$$f(x(t), t) = (8\cos(\sin(5t)) + 3\sin(2t) + 1)\, x^2(t) - 1 = 0. \tag{2.14}$$

The proposed ZD models (2.3), (2.5), (2.7), (2.9), (2.11) and (2.13) with $\gamma = 10$ are exploited to solve the above problem (2.14). Note that the theoretical initial solutions of (2.14) are

$$x^*(0) = \pm\frac{1}{\sqrt{8\cos(\sin 0) + 3\sin 0 + 1}} \approx \pm 0.33.$$

For convenience of observation, we randomly generate the positive and negative initial states $x(0)$, respectively, within $[0.2, 0.5]$ and $[-0.5, -0.2]$, which are the intervals around the theoretical initial solutions ± 0.33. As shown in Fig. 2.5, the neural states of ZD models [denoted by solid curves] converge to the theoretical time-varying inverse square root $x^*(t)$ [denoted by dash–dotted curves] of (2.14) in a short time (about 0.5 s). Therefore, we have substantiated the efficacy of the proposed ZD models for solving the time-varying inverse square root problem with an appropriate value of γ. It is worth pointing out that, even if we set the initial states $x(0) \neq 0$ far away from the theoretical initial solutions ± 0.33, the neural states $x(t)$ of the proposed ZD models (2.3), (2.5), (2.7), (2.9), (2.11) and (2.13) also converge to the theoretical time-varying solutions of (2.14) rapidly.

Example 2.2 In this example, we discuss how the value of design parameter γ affects the convergence performance of the proposed ZD models.

First, let us exploit ZD models (2.3) and (2.7) to solve the following time-varying inverse square root problem with $\gamma = 10$, 100 and 1000, respectively:

$$f(x(t), t) = (2\sin(3t) + 3\exp(\cos(2t)) + 7)\, x^2(t) - 1 = 0. \tag{2.15}$$

Starting with ten randomly-generated initial states $x(0)$, five of which are in $[0.2, 0.3]$ and the others are in $[-0.3, -0.2]$, we have the modeling results of computational error $e(t)$ shown in Fig. 2.6. As seen from the upper graph of Fig. 2.6, the maximal steady-state modeling error of ZD model (2.3) becomes much smaller when the value of design parameter γ increases. Specifically speaking, when $\gamma = 10$, the order of the maximal steady-state modeling error is 10^{-3}; and, when $\gamma = 1000$, the order of the maximal steady-state modeling error decreases to be 10^{-5}. This means that the maximal steady-state modeling error of ZD model (2.3) decreases in an $O(\gamma^{-1})$ manner. Note that the integrator precision (i.e., the relative tolerance of the integrator

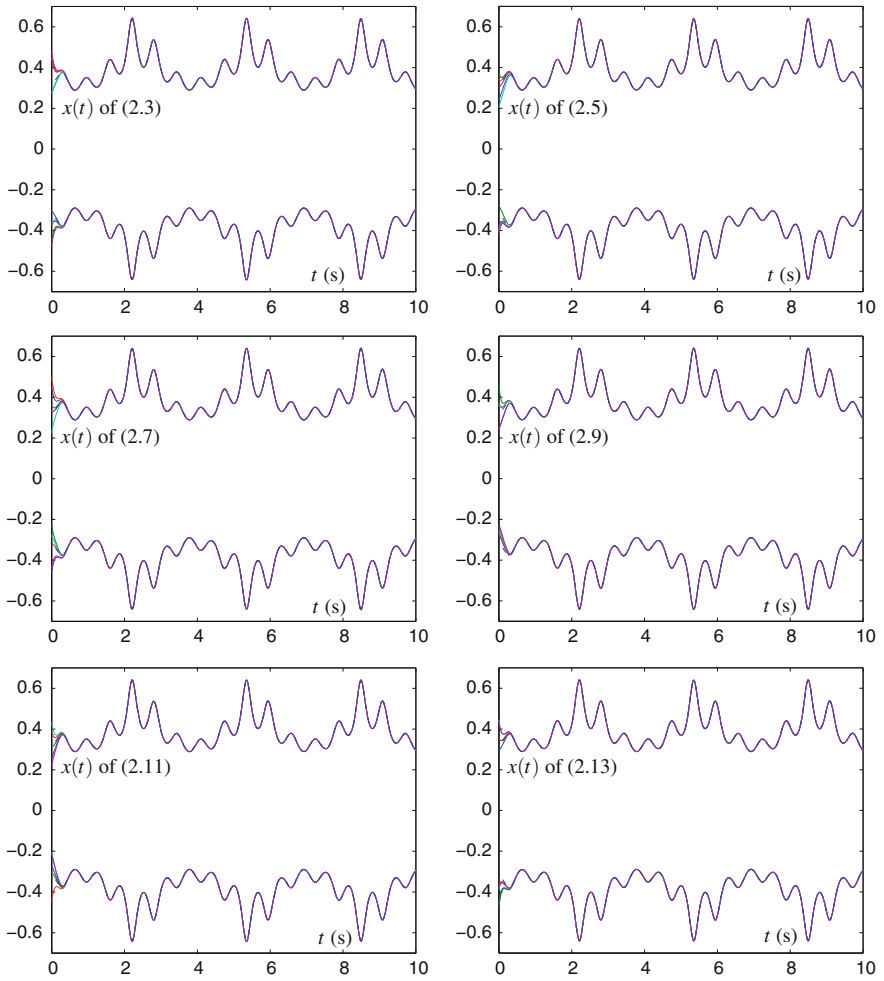

Fig. 2.5 State trajectories of ZD models (2.3), (2.5), (2.7), (2.9), (2.11) and (2.13) with $\gamma = 10$ for solving the time-varying inverse square root problem (2.14)

denoted as RT in this chapter) in the Simulink models also influences the convergence performance and accuracy of the ZD models.

In addition, in the previous modeling results, we set the integrator precision to be 1.0×10^{-5}. Figure 2.7 shows that, when we increase the integrator precision (i.e., decrease RT), the maximal steady-state modeling error of ZD model (2.3) is decreased as well. Theoretically speaking, the maximal steady-state modeling error can decrease to zero, when the relative tolerance RT tends to zero.

Moreover, the convergence speed of the proposed ZD models for solving (2.15) can be expedited effectively by increasing γ. This is shown in the upper and lower graphs of Fig. 2.6 with ZD models (2.3) and (2.7), respectively, as examples. Thus,

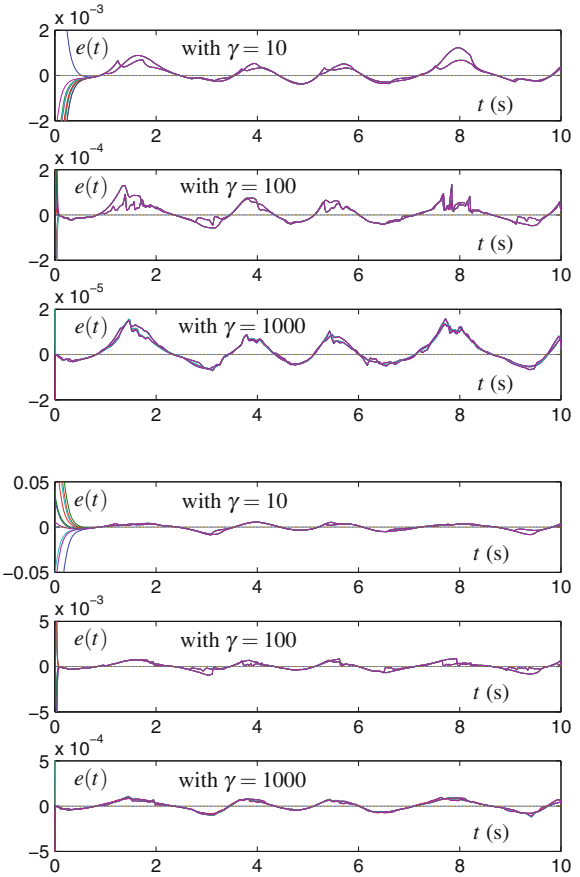

Fig. 2.6 Modeling errors $e(t)$ of ZD models (2.3) and (2.7) with the integrator's relative tolerance being 10^{-5} and with different γ for solving the time-varying inverse square root problem (2.15)

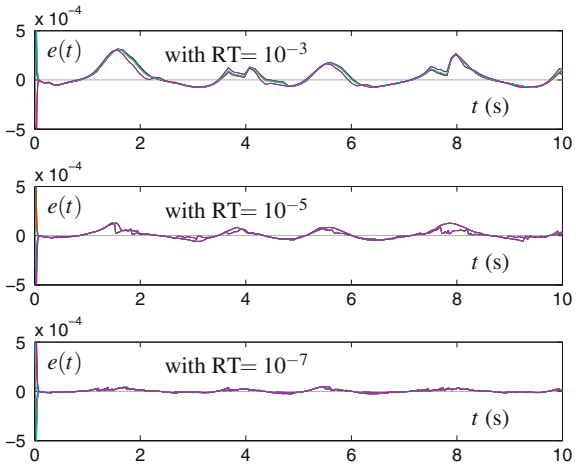

Fig. 2.7 Modeling errors $e(t)$ of ZD model (2.3) with $\gamma = 100$ and with different values of relative tolerance (RT) for solving the time-varying inverse square root problem (2.15)

we should set the value of γ appropriately large not only to decrease the modeling error, but also to shorten the convergence time.

In summary, we have the conclusion that the design parameter γ plays an important role in ZD models (2.3) and (2.7) on the convergence performance (including engineering accuracy). It is worth pointing out that the same conclusion applies to other ZD models [i.e., (2.5), (2.9), (2.11) and (2.13)], whose related modeling results are omitted due to similarity of results. Besides, the modeling tests of ZD models (2.5), (2.9), (2.11) and (2.13) are left to interested readers to complete as a topic of exercise.

2.6 Summary

In this chapter, six different ZD models based on six different ZFs have been proposed, generalized, developed, and investigated for solving the time-varying inverse square root problem in the form of $f(x(t), t) = a(t)x^2(t) - 1 = 0$. In addition, theoretical results and analyses have been given to substantiate the exponential convergence of the proposed ZD models. For possible hardware implementation, the MATLAB Simulink modeling of the proposed ZD models has also been presented and investigated in this chapter. The illustrative modeling results have further substantiated the efficacy of the proposed ZD models on time-varying inverse square root finding.

References

1. Seidel PM (1999) High-speed redundant reciprocal approximation. Integr VLSI J 28(1):1–12
2. Blinn J (2003) Jim Blinn's corner: notation, notation, notation. Elsevier, San Francisco
3. Eberly D (2001) 3D game engine design. Elsevier, San Francisco
4. Clenshaw CW, Olver FWJ (1986) Unrestricted algorithms for reciprocals and square roots. BIT Numer Math 26(4):475–492
5. Lang T, Montuschi P (1999) Very high radix square root with prescaling and rounding and a combined division/square root unit. IEEE Trans Comput 48(8):827–841
6. Pineiro JA, Bruguera JD (2002) High-speed double-precision computation of reciprocal, division, square root, and inverse square root. IEEE Trans Comput 51(12):1377–1388
7. Ercegovac MD, Lang T, Muller JM, Tisserand A (2000) Reciprocation, square root, inverse square root, and some elementary functions using small multipliers. IEEE Trans Comput 49(7):628–637
8. Mead C (1989) Analog VLSI and neural systems. Addison-Wesley Longman, Boston
9. Zhang Y, Yi C, Guo D, Zheng J (2011) Comparison on Zhang neural dynamics and gradient-based neural dynamics for online solution of nonlinear time-varying equation. Neural Comput Appl 20(1):1–7
10. Zhang Y, Leithead WE, Leith DJ (2005) Time-series Gaussian process regression based on Toeplitz computation of $O(N^2)$ operations and $O(N)$-level storage. In: Proceedings of the 44th IEEE international conference on decision and control, pp 3711–3716
11. Zhang Y, Li Z, Xie Y, Tan H, Chen P (2013) Z-type and G-type ZISR (Zhang inverse square root) solving. In: Proceedings of the 4th international conference on intelligent control and information processing, pp 123–128

12. Zhang Y, Li Z, Guo D, Li W, Chen P (2013) Z-type and G-type models for time-varying inverse square root (TVISR) solving. Soft Comput 17(11):2021–2032
13. Zhang Y, Yu X, Xie Y, Tan H, Fan Z (2013) Solving for time-varying inverse square root by different ZD models based on different Zhang functions. In: Proceedings of the 25th Chinese control and decision conference, pp 1358–1363
14. Zhang Y, Guo X, Ma W (2008) Modeling and simulation of Zhang neural network for online time-varying equations solving based on MATLAB Simulink. In: Proceedings of the 7th international conference on machine learning and cybernetics, pp 805–810
15. Tan N, Chen K, Shi Y, Zhang Y (2009) Modeling, verification and comparison of Zhang neural net and gradient neural net for online solution of time-varying linear matrix equation. In: Proceedings of the 4th IEEE conference on industrial electronics and applications, pp 3698–3703
16. Ansari MS, Rahman SA (2011) DVCC-based non-linear feedback neural circuit for solving system of linear equations. Circuits Syst Signal Process 30(5):1029–1045
17. Zhang Y, Yi C (2011) Zhang neural networks and neural-dynamic method. Nova Science Publishers, New York

http://www.springer.com/978-3-662-47333-7

Zhang Functions and Various Models

Zhang, Y.; Guo, D.

2015, XXI, 236 p. 119 illus., 83 illus. in color., Hardcover
ISBN: 978-3-662-47333-7